

ELLIPTIC FLOW DIFFERENCE BETWEEN PARTICLES AND ANTIPARTICLES AND THE EOS OF BARYON-RICH MATTER*

CHE MING KO^a, LIE-WEN CHEN^b, VINCENZO GRECO^c, FENG LI^a
ZI-WEI LIN^d, SALVATORE PLUMARI^c, TAESOO SONG^a, JUN XU^e

^aCyclotron Institute and Department of Physics and Astronomy
Texas A&M University, College Station, TX 77843, USA

^bDepartment of Physics, Shanghai Jiao Tong University, Shanghai 200240, China

^cDipartimento di Fisica e Astronomia, Università di Catania
Via S. Sofia 64, 95125 Catania, Italy

^dDepartment of Physics, East Carolina University

C-209 Howell Science Complex, Greenville, NC 27858, USA

^eShanghai Institute of Applied Physics, Chinese Academy of Sciences
Shanghai 201800, China

(Received February 14, 2014)

We review our recent studies of mean-field effects on the elliptic flows of particles and antiparticles in heavy ion collisions at energies carried out in the Beam Energy Scan (BES) program at the Relativistic Heavy Ion Collider (RHIC). Including mean-field potentials in the hadronic phase of a multiphase transport (AMPT) model, we have found that the elliptic flows are larger for p , K^+ , and π^- than for \bar{p} , K^- , and π^+ , respectively, as observed by the STAR Collaboration. Using a partonic transport model based on the Nambu–Jona-Lasinio (NJL) model, we have also found that the vector mean-field potentials in the baryon-rich quark matter lead to a larger quark than antiquark elliptic flows in these collisions. Using the quark coalescence model to convert quarks and antiquarks to hadrons, we have further found a splitting of the p and \bar{p} , Λ and $\bar{\Lambda}$, and K^+ and K^- elliptic flows with their differences depending on the strength of the quark vector coupling. Our studies have thus demonstrated the possibility of extracting information on the properties of baryon-rich quark–gluon plasma from the BES program at RHIC.

DOI:10.5506/APhysPolBSupp.7.183

PACS numbers: 25.75.-q, 24.10.Lx, 21.30.Fe

* Lecture presented by C.M. Ko at the XXXI Max Born Symposium and HIC for FAIR Workshop “Three Days of Critical Behaviour in Hot and Dense QCD”, Wrocław, Poland, June 14–16, 2013.

1. Introduction

Heavy ion collisions at relativistic energies provide the possibility to study the phase structure of the matter that is described by the quantum chromodynamics (QCD). For the top energy available at RHIC and at the Large Hadron Collider (LHC), the produced quark–gluon plasma (QGP) is nearly baryon free and thus has very small baryon chemical potentials. According to lattice QCD calculations [1–3], the transition from the QGP to the hadronic matter in this region of the phase diagram is a smooth crossover. This phase transition is, however, expected to change to a first-order transition at certain finite baryon chemical potential called the critical point in the QCD phase diagram [4–7]. To probe this region of the QCD phase diagram, the BES program at much lower energies have recently been carried out at RHIC by the STAR Collaboration [8]. Although no definitive signals for a first-order phase transition and the critical end point have been established, a number of interesting results have been observed. One of them is the increasing difference between the elliptic flows of particles and antiparticles as the collision energy decreases. Such a behavior cannot be described by a simple hydrodynamic or hadronic cascade model [9]. Several mechanisms have been proposed to explain this experimental result. These include the different elliptic flows of transported and produced partons during the initial stage of heavy ion collisions [10]; the chiral magnetic effect induced by the strong magnetic field in noncentral collisions [11], the hadronic [12] and the partonic [13] mean-field effects, and the local thermal and baryon chemical equilibrium effect [14]. In the present paper, we review the mean-field effects on the elliptic flows of particles and antiparticles in heavy ion collisions at the BES energies.

2. Hadronic mean-field potentials and elliptical flows

It is known from heavy ion collisions at lower collision energies at SIS/GSI and AGS/BNL that the elliptic flow of nucleons is affected not only by their scattering but also by their mean-field potentials in hadronic matter [15]. Also, the potentials of a particle and its antiparticle are different, and they generally have opposite signs at high densities [16, 17].

For the nucleon and antinucleon potentials, we have taken them from the relativistic mean-field model used in the Relativistic Vlasov–Uehling–Uhlenbeck transport model [18] in terms of the nucleon scalar and vector self-energies. Although the scalar self-energy is attractive for both nucleons and antinucleons, the vector self-energy is repulsive for nucleons and attractive for antinucleons in baryon-rich nuclear matter as a result of the G -parity invariance. Since only light quarks in baryons and antibaryons contribute to the scalar and vector self-energies in the mean-field approach, the potentials

of strange baryons and antibaryons are reduced relative to those of nucleons and antinucleons according to the ratios of their light quark numbers. For kaon and antikaon potentials in the nuclear medium, they are also taken from Ref. [18] based on the chiral effective Lagrangian that fits empirical data on kaon– and antikaon–nucleon scatterings. The resulting potential is then repulsive for a kaon and attractive for an antikaon. The pion potentials are related to their self-energies and have been calculated in Ref. [19] from the pion–nucleon s-wave interaction up to the two-loop order in chiral perturbation theory. In asymmetric nuclear matter, this leads to a splitting of the mean-field potentials for positively and negatively charged pions.

In the absence of antibaryons, the nucleon potential is slightly attractive while that of an antinucleon is strongly attractive, with values of about -60 MeV and -260 MeV, respectively, at normal nuclear matter density of $\rho_0 = 0.16 \text{ fm}^{-3}$. The latter is consistent with those extrapolated from experimental data [20]. Similarly, the K potential is slightly repulsive while the \bar{K} potential is deeply attractive, and their values at ρ_0 are about 20 MeV and -120 MeV, respectively, comparable to those extracted from the experimental data [21]. For pions in neutron-rich nuclear matter, the potential is weakly repulsive and attractive for π^- and π^+ , respectively, and the strength at ρ_0 and isospin asymmetry $\delta = (\rho_n - \rho_p)/(\rho_n + \rho_p) = 0.2$ is about 14 MeV for π^- and -1 MeV for π^+ .

Including these mean-field potentials in the hadronic phase of the string melting AMPT model [22], we have studied the differential elliptic flows of p , K^+ , and π^+ as well as their antiparticles at three different BES energies, and the results are shown in the left window of Fig. 1. Without hadronic potentials the elliptic flows from the AMPT model are similar for particles and their antiparticles. Including hadronic potentials increases slightly the p and \bar{p} elliptic flows at $p_T < 0.5$ GeV/ c , while it reduces slightly (strongly) the p (\bar{p}) elliptic flow at higher p_T . Hadronic potentials also increase slightly the elliptic flow of K^+ while reduces mostly that of K^- . In addition, the effect from the potentials on the elliptic flow decreases with increasing collision energy. The results for the relative p_T -integrated v_2 difference between particles and their antiparticles, defined by $[v_2(P) - v_2(\bar{P})]/v_2(P)$, with and without hadronic potentials are shown in the right window of Fig. 1. These differences are very small in the absence of hadronic potentials. Including hadronic potentials increases the relative v_2 difference between p and \bar{p} and between K^+ and K^- up to about 30% at 7.7 GeV and 20% at 11.5 GeV, but negligibly at 39 GeV. These results are qualitatively consistent with the measured values of about 63% and 13% at 7.7 GeV, 44% and 3% at 11.5 GeV, and 12% and 1% for the relative v_2 difference between p and \bar{p} and between

K^+ and K^- , respectively [8]. Similar to the experimental data, the relative v_2 difference between π^+ and π^- is negative at all energies after including their potentials, although ours have smaller magnitudes.

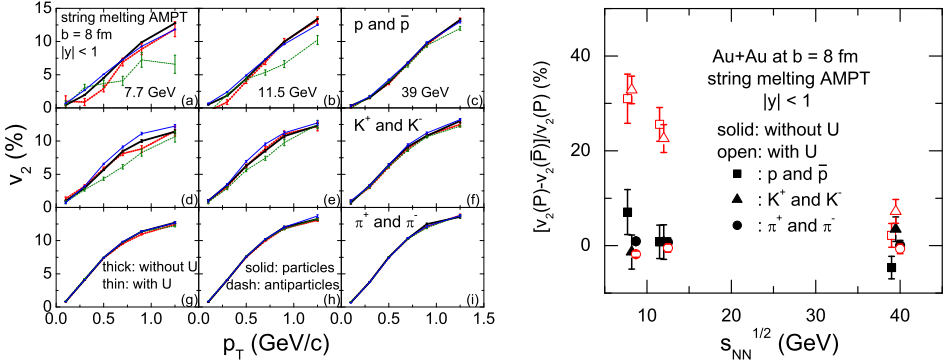


Fig. 1. (Color online) Differential elliptic flows (left window) and relative elliptic flow differences (right window) of mid-rapidity ($|y| < 1$) p and \bar{p} , K^+ and K^- , and π^+ and π^- with and without hadronic potentials in Au+Au collisions at $b = 8$ fm and $\sqrt{s_{NN}} = 7.7, 11.5, \text{ and } 39$ GeV from the string melting AMPT model.

3. Partonic mean fields and elliptic flows

To study the effect of partonic mean fields on parton elliptic flows, we have used in Ref. [13] the NJL model [23, 24], particularly the one for three quark flavors [7]. Like particles and antiparticles in baryon-rich hadronic matter, quarks are affected by attractive scalar and repulsive vector fields, while antiquarks are affected by both attractive scalar and vector fields in baryon-rich quark matter. The value of attractive scalar mean field is related to the difference between current and constituent quark masses, which has a maximum value of about -300 MeV. The magnitude of vector mean-field depends on the product of the quark vector coupling and net-baryon density. For the vector coupling $g_V \sim 17$ MeV fm³ obtained from the Fierz transformation of the quark scalar interaction in the NJL Lagrangian, the vector mean field has a magnitude of 17 MeV if the net-baryon density is 1 fm⁻³, leading to a difference of ≈ 34 MeV in quark and antiquark vector mean fields.

Using the initial quark and antiquark rapidity and transverse momentum distributions in Au+Au collisions at $\sqrt{s_{NN}} = 7.7$ GeV and at impact parameter $b = 8$ fm from the valence quarks and antiquarks converted from hadrons that are obtained from the Heavy-Ion Jet Interaction Generator (HIJING) model [25] through Lund string fragmentation as implemented

in the AMPT model with string melting [22], the effects of partonic mean fields are then studied in a parton transport model. Figure 2 shows the transverse momentum dependence of quark and antiquark v_2 at the end of partonic phase, which is about 1.9 fm/c after the start of the partonic evolution when the energy density in the center of produced quark matter decreases to 0.8 GeV/fm³, for the cases of including only scalar mean field, scalar and time component of vector mean field, scalar and space component of vector mean field, and scalar and both components of vector mean field. For the last case, the difference between the integrated v_2 of up and down quarks and their antiquarks is about 60% of the integrated v_2 of up and down quarks, and that between strange quarks and antistrange quarks is about 29% of the integrated v_2 of strange quarks.

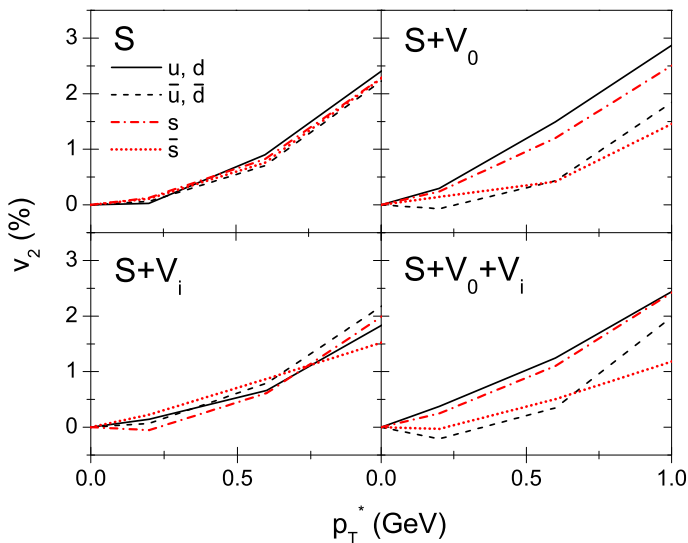


Fig. 2. (Color online) Differential elliptic flows of light and strange quarks and antiquarks at mid-rapidity ($|y| < 1$) at hadronization for the cases of including only scalar mean field (S), scalar and time component vector mean-field ($S + V_0$), scalar and space component vector mean field ($S + V_i$), and scalar and both components of vector mean-field ($S + V_0 + V_i$).

Converting partons to hadrons via the coalescence model [26–28], we show in the left window of Fig. 3 by solid and dashed lines, respectively, the v_2 of p and \bar{p} (left panel), Λ and $\bar{\Lambda}$ (middle panel), and K^+ and K^- (right panel), at hadronization as functions of transverse momentum. It is seen that the quark coalescence leads to a larger hadron v_2 than the quark v_2 at same transverse momentum. Furthermore, the v_2 of p , Λ , and K^- are, respectively, larger than those of \bar{p} , $\bar{\Lambda}$, and K^+ , leading to relative differences

between their integrated v_2 of about 45, 40, and -6.0% , respectively, as shown by solid symbols in the right window of Fig. 3 for $g_v/G = 0.33$, compared with 63 ± 14 , 54 ± 27 , and $13 \pm 2\%$ measured in experiments shown by open symbols in the left-hand side of the figure. The dependence of the relative difference between integrated particle and antiparticle v_2 on the vector coupling g_V is also shown in the right window of Fig. 3 and is seen to increase almost linearly with the strength of vector coupling.

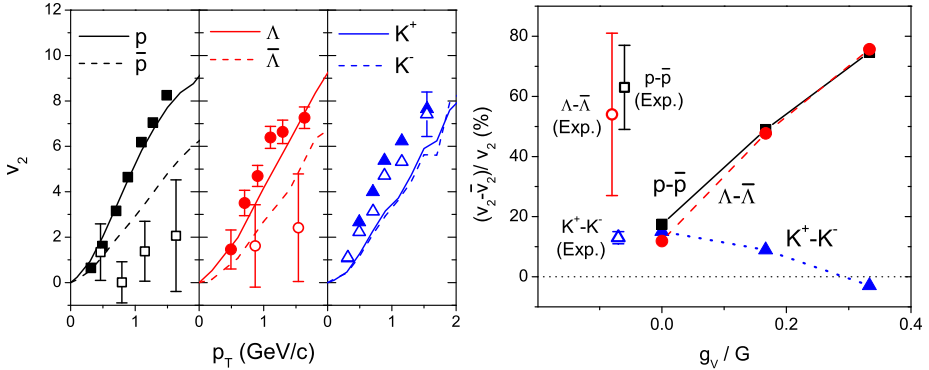


Fig. 3. (Color online) Differential elliptic flows (left window) and relative elliptic flow differences (right window) of midrapidity ($|y| < 1$) p and \bar{p} , Λ and $\bar{\Lambda}$, and K^+ and K^- at hadronization. Experimental data from Refs. [8] are shown by open symbols in the left-hand side of right window.

4. Summary

To summarize, we have studied the elliptic flows of p , K^+ , π^+ and their antiparticles in heavy ion collisions at BES energies by extending the string melting AMPT model to include their mean-field potentials in the hadronic stage. Because of the more attractive \bar{p} than p potentials, the attractive K^- and repulsive K^+ potentials, and the slightly attractive π^+ and repulsive π^- potentials in the baryon- and neutron-rich matter formed in these collisions, smaller elliptic flows are obtained for \bar{p} , K^- , and π^+ than for p , K^+ , and π^- . Also, the difference between the elliptic flows of particles and their antiparticle is found to decrease with increasing collision energy as a result of decreasing baryon chemical potential of hadronic matter. Although these results are qualitatively consistent with the experimental observations, they underestimate the relative elliptic flow difference between p and \bar{p} as well as that between π^- and π^+ and overestimate that between K^+ and K^- .

We have also studied the effect of partonic mean fields on the elliptic flows of quarks and antiquarks in a baryon-rich quark matter by using a transport model based on the NJL model. For the scalar mean field, which

is attractive for both quarks and antiquarks, it leads to a similar reduction of quark and antiquark v_2 as first found in Ref. [29]. The vector mean field, on the other hand, has very different effects on quarks and antiquarks in the baryon-rich matter as it is repulsive for quarks and attractive for antiquarks. The time component of vector mean field turns out to have the strongest effect, resulting in a significant splitting of the quark and antiquark v_2 as a result of enhanced quark v_2 and suppressed antiquark v_2 . Using the quark coalescence model, we have further studied the elliptic flows of p , Λ , and K^+ and their antiparticles produced from the baryon-rich quark matter and found that the differences between particle and antiparticle elliptic flows are appreciable as a result of different quark and antiquark v_2 . The magnitude of the relative integrated v_2 difference between particles and their antiparticles depends on the strength of vector coupling. Although using a larger vector coupling in the partonic matter can describe the p and \bar{p} as well as the Λ and $\bar{\Lambda}$ relative v_2 differences that were measured in experiments by the STAR Collaboration [8], it fails to reproduce the measured relative v_2 between K^+ and K^- . This is not surprising since other effects that can lead to the splitting of the elliptic flows of particles and their antiparticles have not been included in our study. Although a quantitative determination of the partonic vector interaction requires a more complete study, the present study has clearly shown that the splitting of quark and antiquark elliptic flows and thus that of particles and their antiparticles is sensitive to the strength of partonic vector interaction. Our results, therefore, indicate for the first time that studying the elliptic flow in heavy ion collisions at BES energy can potentially allow for the determination of the partonic vector interaction in baryon-rich QGP and thus the equation of state of QGP at finite baryon chemical potential.

Based on work supported in part by the U.S. National Science Foundation under grant No. PHY-106857, the Welch Foundation under grant No. A-1358, the ERC-StG under the grant QGPDyn No. 259684, the NNSF of China under grant Nos. 10975097 and 11135011, Shanghai Rising-Star Program under grant No. 11QH1401100, “Shu Guang” project supported by the Shanghai Municipal Education Commission and Shanghai Education Development Foundation, and the ERC-StG under the grant QGP-Dyn No. 259684, the Major State Basic Research Development Program in China (No. 2014CB845401), the “Shanghai Pujiang Program” under grant No. 13PJ1410600, and the “100-talent plan” of Shanghai Institute of Applied Physics under grant Y290061011 from the Chinese Academy of Sciences.

REFERENCES

- [1] C. Bernard *et al.* [MILC Collaboration], *Phys. Rev.* **D71**, 034504 (2005).
- [2] Y. Aoki *et al.*, *Nature* **443**, 675 (2006).
- [3] A. Bazavov *et al.*, *Phys. Rev.* **D85**, 054503 (2012).
- [4] M. Asakawa, K. Yazaki, *Nucl. Phys.* **A504**, 668 (1989).
- [5] K. Fukushima, *Phys. Rev.* **D77**, 114028 (2008) [*Erratum ibid.*, **D78**, 039902 (2008)].
- [6] S. Carignano, D. Nickel, M. Buballa, *Phys. Rev.* **D82**, 054009 (2010).
- [7] N.M. Bratovic, T. Hatsuda, W. Weise, [arXiv:1204.3788](https://arxiv.org/abs/1204.3788) [hep-ph].
- [8] L. Adamczyk *et al.* [STAR Collaboration], *Phys. Rev.* **C86**, 054908 (2012).
- [9] V. Greco, M. Mitrovski, G. Torrieri, *Phys. Rev.* **C86**, 044905 (2012).
- [10] J.C. Dunlop, M.A. Lisa, P. Sorensen, *Phys. Rev.* **C84**, 044914 (2011).
- [11] Y. Burnier, D.E. Kharzeev, J. Liao, H.-U. Yee, *Phys. Rev. Lett.* **107**, 052303 (2011).
- [12] J. Xu, L.-W. Chen, C.M. Ko, Z.-W. Lin, *Phys. Rev.* **C85**, 041901 (2012).
- [13] T. Song *et al.*, [arXiv:1211.5511](https://arxiv.org/abs/1211.5511) [nucl-th].
- [14] J. Steinheimer, V. Koch, M. Bleicher, *Phys. Rev.* **C86**, 044903 (2012).
- [15] P. Danielewicz, R. Lacey, W.G. Lynch, *Science* **298**, 1592 (2002).
- [16] C.M. Ko, G.Q. Li, *J. Phys. G* **22**, 1673 (1996).
- [17] C.M. Ko, V. Koch, G.Q. Li, *Annu. Rev. Nucl. Part. Sci.* **47**, 505 (1997).
- [18] G.Q. Li, C.M. Ko, X.S. Fang, Y.M. Zheng, *Phys. Rev.* **C49**, 1139 (1994).
- [19] N. Kaiser, W. Weise, *Phys. Lett.* **B512**, 283 (2001).
- [20] E. Friedman, A. Gal, J. Mareš, *Nucl. Phys.* **A761**, 283 (2005).
- [21] E. Friedman, A. Gal, J. Mareš, A. Cieplý, *Phys. Rev.* **C60**, 024314 (1999).
- [22] Z.W. Lin *et al.*, *Phys. Rev.* **C72**, 064901 (2005).
- [23] Y. Nambu, G. Jona-Lasinio, *Phys. Rev.* **122**, 345 (1961).
- [24] Y. Nambu, G. Jona-Lasinio, *Phys. Rev.* **124**, 246 (1961).
- [25] M. Gyulassy, X.-N. Wang, *Comput. Phys. Commun.* **83**, 307 (1994).
- [26] V. Greco, C.M. Ko, P. Levai, *Phys. Rev. Lett.* **90**, 202302 (2003); *Phys. Rev.* **C68**, 034904 (2003).
- [27] V. Greco, C.M. Ko, R. Rapp, *Phys. Lett.* **B595**, 202 (2004).
- [28] L.-W. Chen, C.M. Ko, B.-A. Li, *Phys. Rev.* **C68**, 017601 (2003); *Nucl. Phys.* **A729**, 809 (2003).
- [29] S. Plumari *et al.*, *Phys. Lett.* **B689**, 18 (2010).